ELSEVIER

Thermochimica Acta 310 (1998) 53–60

thermochimica acta

Heat conduction, convection and radiolysis of the H_2/O_2 system in the water absorbed dose calorimeter[1]

A. Krauss*, M. Roos

Physikalisch-Technische Bundesanstalt (PTB), Fachlabor 6.23, Bundesallee 100, D-38116 Braunschweig, Germany

Received 12 May 1997; accepted 16 June 1997

Abstract

The calorimeter allows the water absorbed dose, a measure of radiotherapy, to be measured according to its definition. Different detector types are used in the PTB calorimeter; this paper discusses heat conduction, convection and the radiolysis of the H_2/O_2 system for a 'sealed' detector. The 'sealed' detector allows the calorimeter to be operated at room temperature in the case of ^{60}Co-γ-radiation. © 1998 Elsevier Science B.V.

Keywords: Convection; Diffusion; Heat conduction; Radiolysis; Water absorbed dose calorimeter

1. Introduction

The quantity of water absorbed dose, D_w, is a measure of dosimetry in radiation therapy. According to its definition as the quotient of $d\varepsilon/dm$, where $d\varepsilon$ is the mean energy imparted by ionizing radiation to water of the mass dm at the point of measurement, a water-absorbed dose calorimeter [1] can be used to determine this quantity with high accuracy and, basically, without any energy-dependent conversions or corrections. From the radiation-induced temperature rise, ΔT, at a point in a water phantom, the water-absorbed dose is given by the equation:

$$D_w = \Delta T \times c_p \times 1/(1-h)$$

where c_p is the specific heat capacity of water and h the so-called heat defect which is the relative difference between the radiation energy imparted to water and the energy occurring as heat. The heat defect is due to the overall exothermicity or endothermicity of chemical reactions initiated by the radiolysis of water. It can be determined by an independent experimental method and by means of numerical simulation of the radiolysis [2–5].

Due to heat transport effects, the water calorimeter should preferably be applied under irradiation conditions without steep dose gradients and pronounced curvature of the dose distribution in the vicinity of the point of measurement. The influence of convection in the water must be negligible [6], and the influence of heat conduction should be minimized by a proper design, allowing an adequate correction, for example by finite element calculations.

At PTB, a water calorimeter was developed [1,2,7,8,11] as a primary standard for the unit of water-absorbed dose at ^{60}Co-γ-radiation. It is operated at a water temperature of 4°C to avoid convection. The amount of non water-equivalent material in the vici-

*Corresponding author. Fax: 00 49 0531 5926405.

[1]Presented at the Twelfth Ulm-Freiberg Conference, Freiberg, Germany, 19–21 March 1997

PII S0040-6031(97)00385-7

nity of the thermistors is minimized ('open' detector). As a result, the perturbation of the radiation field is almost negligible, and the selective heating by the irradiation of materials with specific heat capacities and radiation interaction coefficients deviating from those of water ('excess heat') is also negligible.

Furthermore, a second type of calorimeter was developed, which is less complex, so that it can be applied as a transfer standard for therapeutical photon, electron and proton beams. The detector consists of two thermistors embedded in thin glass pipettes which are mounted inside a water-filled glass cylinder ('sealed' detector) [9,10]. Since the water inside the cylinder is almost exclusively in contact with carefully cleaned glass, the amount of impurities in the water from the vessel surface is reduced, facilitating the specification of the water quality. Therefore, this calorimeter type is well suited for testing numerical simulations of the radiolysis of water by performing benchmark experiments at different temperatures and for different water qualities inside the cylinder.

In dependence on the preparation of the water in the glass cylinder, the corresponding radiation-induced chemical reactions can lead to a spatially dependent energy balance (i.e. heat defect) inside the glass cylinder, causing strong temperature gradients. In turn, heat conduction and diffusion effects then can have an additional influence on the results of the caloric measurement.

In the present paper, heat transport as well as diffusion effects are discussed and experimentally investigated.

2. Experimental

The principle of the water absorbed dose calorimeter as well as some design features were described previously [1,2,6,7,11]. The calorimeter essentially consists of a water-filled perspex tank $30\times30\times30\ cm^3$ in size, which is placed inside a thermally insulated container. To operate the calorimeter at 4°C, this container is placed inside a second, larger container with active temperature stabilization. During irradiation in an extended horizontally directed ^{60}Co-γ-radiation field, the typical temperature increase at the point of measurement is of the order 0.5 mK, which can be measured with a relative standard deviation of the mean of about 0.1% with respect to the measurements of one day.

The 'sealed' detector is based on the development by Domen [9] and consists of a glass cylinder (diameter 40 mm, length 110 mm) having a wall thickness of about 0.3 mm. Two glass capillaries (length 100 mm) are mounted through the front side of the cylinder so that the opposing capillary ends are situated at a distance of about 10 mm. The end section of each capillary has a diameter of less than 0.5 mm and contains a thermistor of 0.25 mm in diameter. To ensure thermal coupling, the thermistors are embedded in epoxy over a length of about 1.5 mm. The capillary ends are closed by a glass seal. A photograph of the detector is shown in Fig. 1. The detector is fixed inside the larger water phantom of the calorimeter in such a way that the cylinder axis of the detector is parallel to the radiation entrance window.

Inside the large water phantom of the calorimeter, singly distilled water is used. The water which is filled into the cylinder can be specially prepared, for example by saturation with different gases or gas mixtures. It is taken from a recirculating water purification system (Seralpur Delta UV/UF), consisting of an entrance filter unit, two ion-exchange columns, and an UV unit (wavelength 185 and 254 nm) in combination with an ultrafiltration unit for the oxidization and removal of organic impurities. This system delivers high purity water at a flowrate of 90 l/h with a conductivity of less than 0.055 μS/cm. By means of a glass bottle with a fritted disk inside and two calibrated mass flowmeters (MKS 1159B), the water is then saturated with a gas mixture of H_2 and O_2. The flow ratio of the gases is adjusted to obtain a concentration (related to the solubility of the gases) of 0.076 mmol/l for oxygen and 0.80 mmol/l for hydrogen at 20°C. By means of a galvanic oxygen probe (WTW CellOx 325), which offers 0.01 mg/l resolution and 0.5% accuracy, the O_2 concentration can be directly determined.

The distance between the ^{60}Co-γ-source (dose rate about 0.01 Gy/s) and the surface of the water phantom of the calorimeter was 100 cm, and the diameter of the horizontally directed circular field at the phantom surface was 259 mm. Caloric measurements were

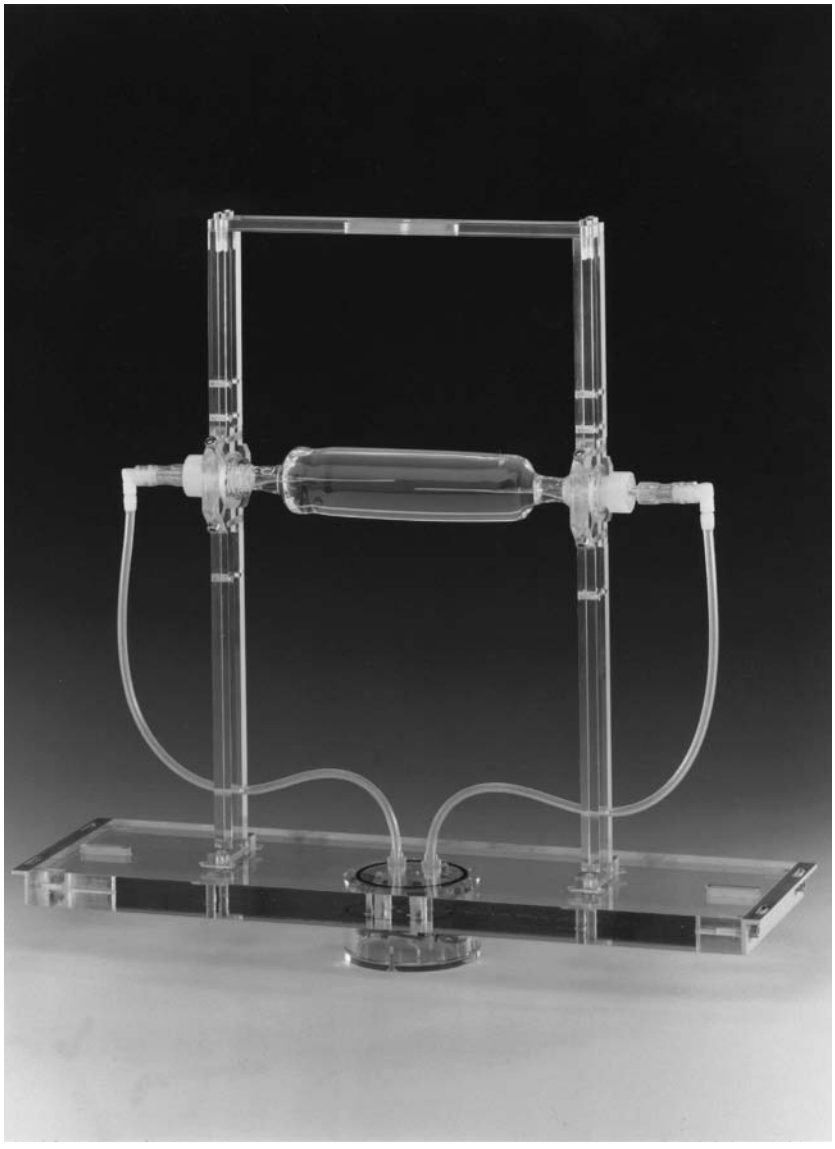

Fig. 1. Photograph showing the 'sealed' detector fixed in a support structure.

performed inside the water phantom at a depth of 5 cm. For the investigation of convection, experiments were carried out at water temperatures of 4 and 20°C and with thermistor electrical powers between 15 and 120 μW. All other experiments were performed at 20°C with the thermistors having 15 μW electrical power.

3. Results and discussion

3.1. Heat conduction effects

In the present paper, those heat conduction effects are investigated which are due to excess heat in non-water materials or temperature gradients produced by

the radiolysis of water. Heat conduction effects caused by the initial radiation-induced temperature profile in water (corresponding to the dose profile) and by the difference of the heat defect outside and inside the detector were investigated previously [8,9].

3.1.1. Excess heat

In the vicinity of the temperature sensors of the 'sealed' detector, a larger amount of material is to be found, which have specific heat capacities and radiation interaction parameters differing from those of water. During irradiation, the rate of the temperature increase in these materials is greater than in the surrounding water, i.e. excess heat is produced. Due to heat transport, the temperature difference between water and non-water materials reaches a constant value depending on the geometry, the specific heat capacities, the mass energy absorption coefficients, the mass stopping powers, the thermal diffusivities of the irradiated materials and the dose rate of irradiation. When irradiation is stopped, the temperature difference is eliminated by heat conduction. This is shown in Fig. 2.

A steeper temperature rise can be seen just after the start of irradiation, leading to a temperature difference between temperature sensor and water of about 8 μK. Within less than 10 s after irradiation is stopped, this temperature difference is vanished. For a correct analysis of the caloric measurement, the extrapolation of the post-irradiation period to the mid-run position therefore must not start directly after irradiation is switched off. Whereas this 'direct' effect of the selective heating of the thermistors is clearly visible, the influence of the excess heat from the cylinder and from the support by heat transport is lessened so that in the case of this detector no pronounced structures are produced during irradiation and the post-irradiation period. Nevertheless, this effect has also to be taken into account. For the application of this calorimeter as a transfer standard, it is advantageous to select equal dose rates and irradiation periods so that the influences on the calibration and on measurements tend to cancel each other. In the example shown, the excess heat and the influences on the post-irradiation period are kept small essentially by thin glass walls of the thermistor holders and by the long distance from their support.

More robust detectors require, for instance, thicker glass capillaries producing more excess heat in the vicinity of the thermistors. In this case, heat conduction from the support of the thermistors at the glass cylinder and from the cylinder itself is increased. The excess heat of these more distant parts therefore affects the signal of the thermistors and influences a larger part of the calorimeter post-irradiation period. In this case, it is of particular importance that all parameters of the geometry can be well defined, allowing a correction of the caloric measurement by means of finite-element calculations.

3.1.2. Effects due to the radiolysis

For the numerical simulations of the radiolysis of water, the G-values and rate constants of a number of chemical reactions must be known [4,5,12,13]. In order to describe the radiolysis of the aqueous H_2/O_2 system used in this investigation, numerical simulations were carried out, allowing for the kinetics of about 50 different chemical reactions. The simulations are based on the numerical solution of a set of coupled first-order differential equations for up to 22 different reaction products. The resulting heat defect is calculated from the total change in the concentration of these products and during irradiation with ^{60}Co-γ-radiation, the aqueous H_2/O_2 system is characterized by a stable stationary state with zero heat defect after an absorbed dose of about 272 Gy. Before the stationary state is reached, H_2 and O_2 are exothermally converted into H_2O_2, resulting in a smooth increase in the heat defect with absorbed dose. When the O_2 concentration is consumed, the H_2O_2 is decomposed into water within an absorbed dose range of about 12 Gy, which leads to a strong exothermal 'peak' structure in the heat defect (solid line (———) in Fig. 3).

According to a dose gradient for ^{60}Co-γ-radiation of about 0.5% mm^{-1} at a water depth of 5 cm, the H_2O_2 'peak' structure corresponds to a geometric spread of less than 10 mm. Therefore, further irradiation is equivalent to a shift of the 'peak' structure through the cylinder (along the beam direction). Because the thermistors are located in the middle of the cylinder, the caloric measurements are influenced by heat conduction effects, which depend on the H_2O_2 heat source distribution relative to the thermistors. Fig. 3 shows the comparison of the calculated heat defect for the H_2O_2 system with the experimental results; the mean value of the experimental results

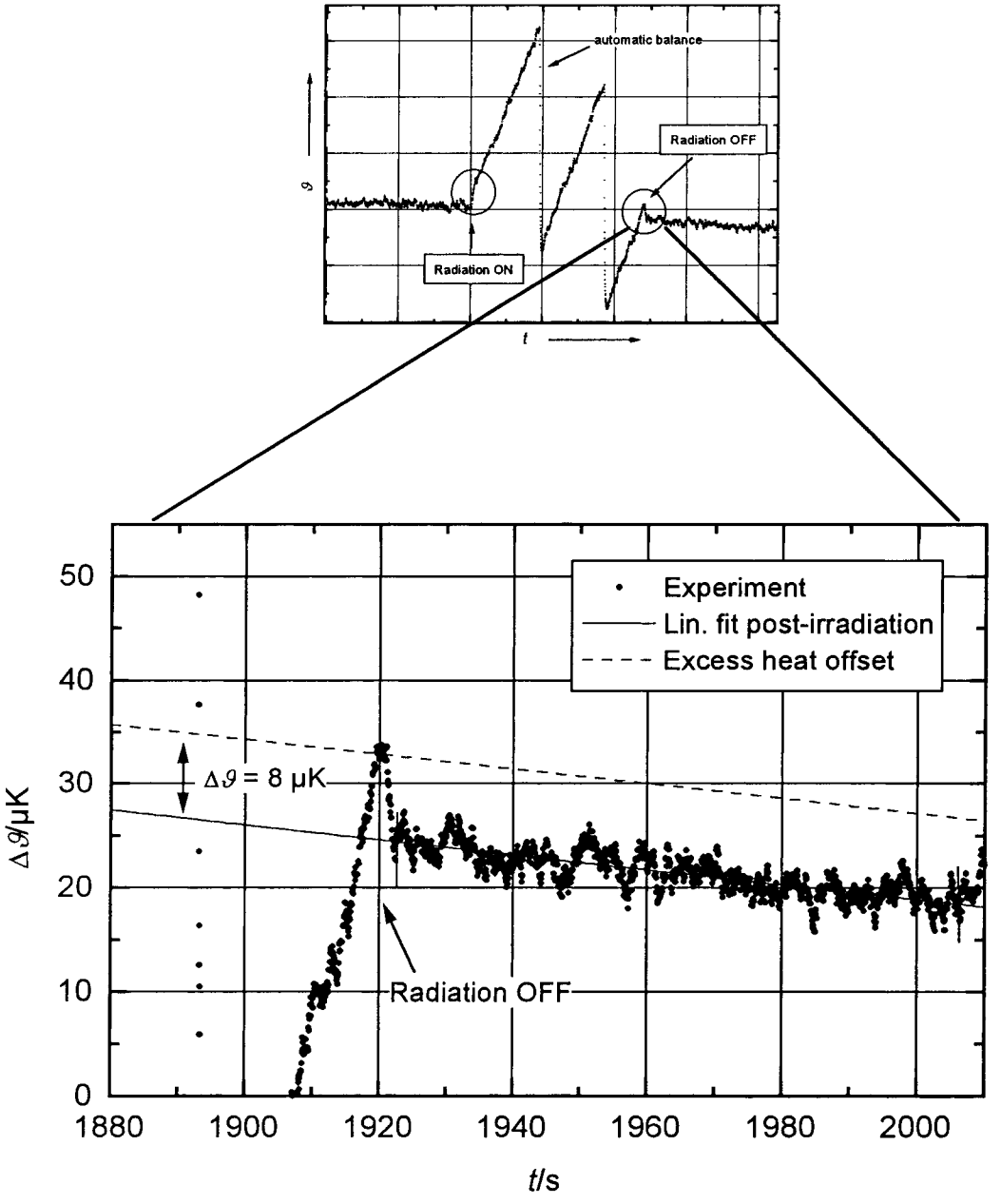

Fig. 2. Temperature T as a function of time t during a typical caloric measurement (upper part). The lower part of the figure shows the influence of excess heat at the time when irradiation ends.

in the stationary state behind the H_2O_2 peak was normalized to a heat defect value of h=0. In the lower part of Fig. 3, the peak region of the heat defect is presented on a larger scale. The dashed line (- - -) shows the apparent heat defect when the heat conduction of the undisturbed system (i.e. without non-water components) is taken into account in the numerical calculations, constituting a first-order approximation

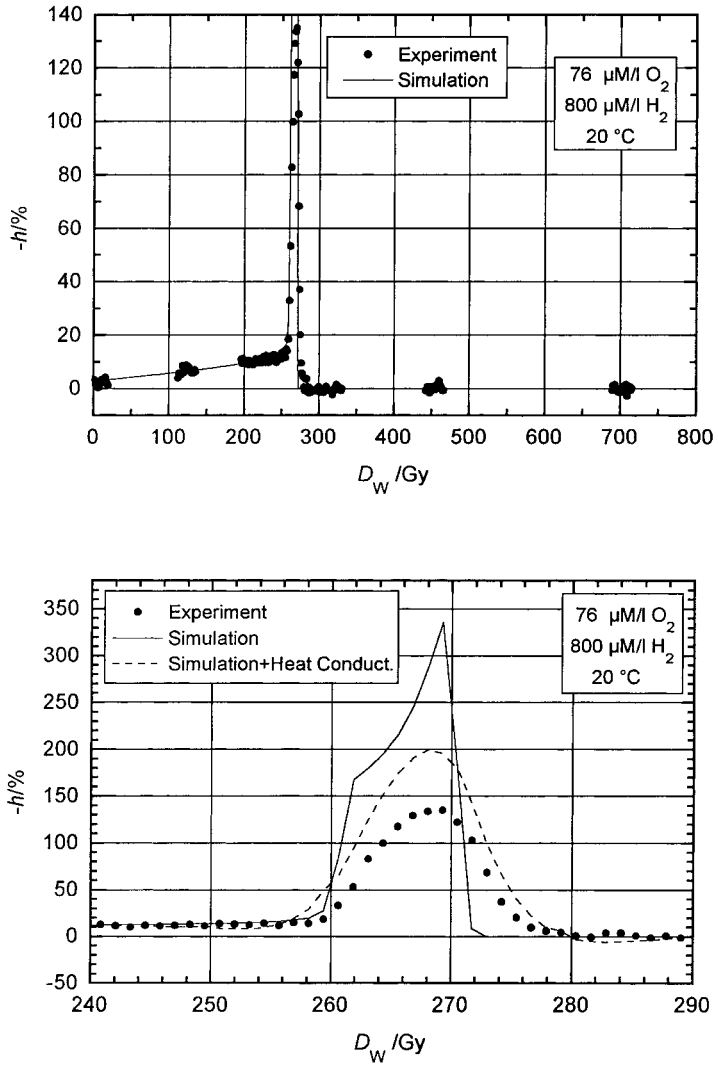

Fig. 3. The exothermal heat defect $-h$ as a function of the absorbed dose D_w. Comparison between caloric measurement and numerical simulation for the H_2/O_2 system in the absorbed dose range up to 800 Gy (upper part). The lower part shows the theoretical heat defect curve in the 'peak' region (———), the theoretical curve after correction for the heat conduction in the undisturbed system (- - -), and the experimental values (●).

of the apparent heat defect in the experiment (circles (●)).

3.2. Diffusion

If the dose gradient in the surroundings of the thermistors leads to a gradient in the concentration of radiolytic reaction products, the calorimeter results may have been influenced by diffusion processes. Although the speeds of diffusion processes are rather low, they can be significant if the concentration gradients are steep or if the time intervals are large. In the case of the radiolysis of the H_2O_2 system, the concentration of the H_2O_2 drops from about 60 µmol/l to zero within a distance of about 10 mm. Using tabulated values for the diffusion coefficient of H_2O_2 in water [12] and applying Fick's laws of diffusion, it can be shown that for the dose-to-time course for succes-

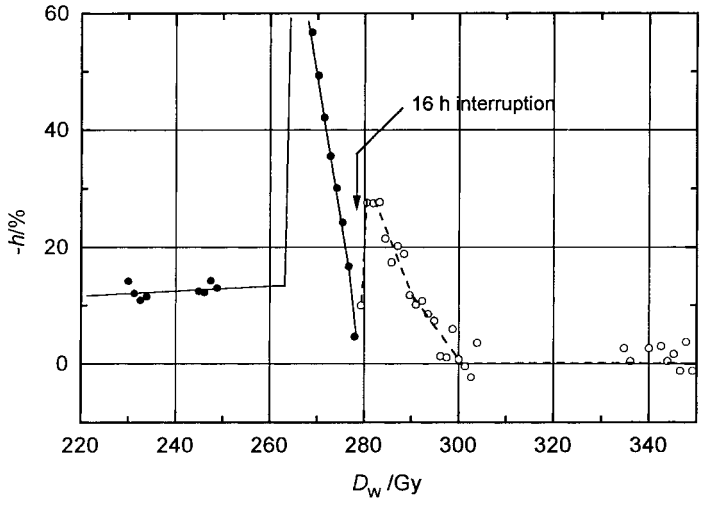

Fig. 4. The exothermal heat defect $-h$ as a function of the absorbed dose D_w for an experiment which was interrupted for 16 h during the H_2O_2-destruction. The figure shows the lower part of the H_2O_2 peak. The solid circles (●) represent the experimental values before the interruption, the open circles (○) the experimental values after the interruption; the lines are to guide the eye.

sive caloric measurements in this investigation, the influence of the diffusion is negligible. But if the dose-to-time programme is modified, the influence may be important. This is demonstrated by an interruption of the series of irradiations during the H_2O_2 destruction. At the time the irradiations were interrupted, not all of the H_2O_2 in the glass cylinder was destroyed. Over an interval of 16 h, diffusion slightly increases the concentration of H_2O_2 at the position of the thermistors. Further irradiations result in a higher heat defect as compared to the measurements taken 16 h earlier. This is shown in Fig. 4.

3.3. Convection

Temperature gradients in the water can lead to convection if the so-called Rayleigh number exceeds a value of about 1000 [14]. The Rayleigh number depends (among other parameters) directly on the volumetric expansion coefficient of water and on the cube of the distance of mechanical convection barriers. The onset of convection can therefore be avoided by operating the calorimeter at a temperature of 4°C or by means of convection barriers [6]. For the 'sealed' detector, the diameter of the glass cylinder has been chosen such that the wall itself forms a mechanical barrier to convection at room temperature. If convection occurs in the water within the detector cylinder during a measurement, it will disturb the radiation-induced temperature distribution, resulting in unpredictable and sudden changes in the calorimeter pre- and post-irradiation periods.

The effectiveness of the cylinder as a mechanical convection barrier was proved by comparing the results of measurements at room temperature with those of measurements at 4°C. As a measure of the influence of convection on the caloric results, the relative standard deviation of the measured temperature increase for a large number of measurements (about 50 for each temperature) was chosen. Because of a large temperature gradient between thermistor and water due to the electrical power of the thermistors (about 1.3 mK/μW), measurements with high thermistor power should detect even smallest convective motions in the water. Caloric measurements were therefore also performed for different values of the thermistor power between 15 and 120 μW. It turns out that the standard deviation of the results obtained at room temperature is slightly greater than for the 4°C measurements. On the other hand, there is no significant dependence on the thermistor power. This means that – according to theoretical expectations – there are no substantial convection effects inside the detector cylinder, since its dimensions keep the Rayleigh number below the critical value.

This is, however, not true for the large water phantom surrounding the detector cylinder. Due to its larger dimensions, the radiation-induced temperature differences may be large enough to raise the Rayleigh number above the critical value. Caused by the low thermal diffusivity of the water, the effect of the resulting convection on the temperature of the thermistors surrounded by the stagnant water inside the glass cylinder is strongly lessened. It usually results in slightly less stable calorimeter pre- and post-irradiation periods. Therefore, in the case of ^{60}Co-γ-radiation, it is – also in the case of horizontally directed beams – usually sufficient to operate the calorimeter with the sealed detector at room temperature.

4. Conclusions

Heat conduction, convection and diffusion effects were investigated for the water calorimeter with sealed detector. The excess heat does not constitute a problem for the application of this calorimeter if the detector is of the Domen type, i.e. the amount of material in the vicinity of the thermistors and the heat conduction from the surrounding glass cylinder are minimized. Nevertheless, this effect has to be taken into account. In the case of more robust detectors, an additional increase in the measuring uncertainty is unavoidable. In any case, the perturbation of the radiation field has to be taken into account; the corrections may be determined by means of the calorimeter used with the open detector. Furthermore, it turns out that – also in the case of horizontally directed ^{60}Co-γ-beams – convection inside the detector cylinder is sufficiently suppressed and that the effect of convection in the phantom outside is lessened to such a degree that this calorimeter can be used at room temperature. The same applies to various radiation beams which cause similar dose distributions in the phantom.

References

[1] S.R. Domen, J. Res. Nat. Bur. Stand. 87(3) (1982) 211–235.
[2] A. Krauss, M. Roos, Thermochim. Acta 229 (1993) 125–132.
[3] M. Roos, in: C.K. Ross, N.V. Klassen (Eds.), NRC Workshop on Water Calorimetry, NRC Publication 29637, Ottawa, 1988, p. 77.
[4] J.W. Fletcher, Radiation Chemistry of Water at Low Dose Rate, Emphasis on the Energy Balance, AECL-7834, Chalk River Nuclear Laboratories, Chalk River, Ontario, 1982.
[5] N.V. Klassen, C.K. Ross, Radiat. Phys. Chem. 38(1) (1991) 95.
[6] S.R. Domen, A. Krauss, M. Roos, Thermochim. Acta 187 (1991) 225–233.
[7] M. Roos, in: C.K. Ross, N.V. Klassen (Eds.), NRC Workshop on Water Calorimetry, NRC Publication 29637, Ottawa, 1988, p. 9.
[8] M. Roos, Thermochim. Acta 119 (1987) 81–93.
[9] S.R. Domen, J. Res. Natl. Stand. Technol. 99 (1994) 121.
[10] H. Palmans, J. Seuntjens, in NPL Calorimetry Workshop, Teddington, 1994.
[11] A. Krauss, M. Roos, in NPL Calorimetry Workshop, Teddington, 1994.
[12] A.J. Elliot, Rate Constants and G-Values for the Simulation of the Radiolysis of Light Water over the Range 0–300°C, AECL-11073, Chalk River Nuclear Laboratories, Chalk River, Ontario, 1994.
[13] N.V. Klassen, C.K. Ross, K.R. Shortt, in NPL Calorimetry Workshop, Teddington, 1994.
[14] E. McLaughlin, Chem. Rev. 64 (1964) 389–428.